Synthesis and Evolution of Novel Hollow ZnO Urchins by a Simple Thermal Evaporation Process

Guozhen Shen,*,†,‡ Yoshio Bando,† and Cheol-Jin Lee*,‡

Advanced Materials Laboratory, National Institute for Materials Science, Namiki 1-1, Tsukuba, Ibaraki 305-0044, Japan, and Department of Nanotechnology, Hanyang University, 17-Haengdang-dong, Seongdong-gu, Seoul 133-791, Korea

Received: March 3, 2005; In Final Form: April 3, 2005

Delicate hollow ZnO urchins have been fabricated by thermal evaporation of metallic zinc powders in a tube furnace without the use of additive, high temperature, or low pressure. The phase transformation, morphologies, and photoluminescence evolution of the ZnO products were carefully studied and investigated with X-ray diffraction (XRD), scanning electron microscopy (SEM), high-resolution transmission electron microscopy (HRTEM), selected area electron diffraction (SAED), and photoluminescence (PL) spectra. These studies indicated that the growth of hollow ZnO urchins involves the vaporization of Zn powder, solidification of liquid droplets, surface oxidation, sublimation, and self-catalytic growth of one-dimensional nanowires.

Introduction

In recent years, synthesis and assembly of inorganic materials with specific size, phase, composition, and morphology have attracted intensive interest because of the potential to design new materials and devices in various fields such as catalysis, medicine, electronics, cosmetics, etc.[1,2] Many efforts have focused on the integration of one-dimensional (1-D) nanoscale building blockes into two- and three-dimensional (2-D, 3-D) ordered superstructures or complex functional architectures, which is a crucial step toward realization of functional nanosystems.[3,4] In addition to common 1-, 2-, and 3-D architectures, controlled organization of primary building unites into curved structures represents another challenge for materials self-assembly, as hollow structures are highly demanded in new technological applications.[5,6]

As an important wide band-gap semiconductor with a band-gap of 3.37 eV and large excitation binding energy of 60 meV at room temperature, zinc oxide (ZnO) has stimulated a wide range of research interest. It is a versatile smart material that has unique applications in catalysts, sensors, piezoelectric transducers and actuators, and photovoltaic and surface acoustic wave devices. ZnO is also a biosafe and biocompatible material, and can be directly used for biomedical applications without coating.[7,8] Since Yang et al. reported ZnO nanowire array nanolasers,[8] synthesis and assembly of ZnO with different forms of controlled nanostructures have been widely explored in recent years and many kinds of interesting and delicate ZnO nanostructures have been obtained by using different methods based on vapor phase processes and solution processes.[9−16] Among these methods, the vapor transport and condensation process proved to be an effective route to synthesize ZnO nanostructures including ZnO nanorings,[9] tower-like structures,[10] nanowire−nanoribbon junction arrays,[11] hierarchical ZnO nanosructures with 6-, 4-, and 2-fold symmetries,[12] nanobridges and nanonails,[13] mesoporous polyhedral cages and shells,[14] and so on. To get these kinds of nanostructures, usually additives such as SnO_2, In_2O_3, In, etc., very high temperature, or extremely low pressure are required. Invention of a simple method to obtain novel ZnO nanostructures is still a big challenge to chemists and material scientists.

Herein, we report a very simple atmospheric pressure thermal evaporation route to grow novel hollow ZnO urchins without use of additive, high temperature, or low pressure. The process is based on thermal evaporation of metallic zinc powder in a tube furnace at 750 °C. We used zinc powder because Zn vapor pressure can reach up to 10.8 Pa at a temperature down to 400 °C, which avoided the use of high temperature.[17] The structures of the hollow ZnO urchins are studied and a growth mechanism is proposed.

Experimental Section

The 3-D hollow ZnO urchins were synthesized by using a very simple thermal evaporation process without catalyst. The experimental apparatus includes a horizontal tube furnace with Ar gas supply system. Metallic zinc powders (100 mesh, 99.998%) acquired from Sigma-Aldrich were used as source materials. In a typical experiment, a p-type silicon substrate was etched with use of hydrofluoric acid for 30 s and cleaned ultrasonically with ethanol and deionized water in sequence and then dried at room temperature. Zn powder (0.065 g) was loaded into an alumina boat and placed in the center of an quartz tube in a horizontal tube furnace. The silicon substrate was located about 7 cm downstream from the source. The tube was heated to 750 °C and held at this temperature for 10−60 min under a constant flow of 500 sccm argon. The furnace was then shut down and cooled to room temperature under an Ar flow.

The products were characterized by scanning electron microscopy (SEM, Hitachi S-4700) and transmission electron microscopy (TEM, Tecnai F20) and selected area electron diffraction (SAED). The X-ray diffraction spectrum (XRD) was obtained on a Rigaku DMAX 2500 diffractometer. Photoluminescence (PL) was measured at room temperature, using a 325 nm He−Cd laser as the excitation light source.

Results and Discussion

After thermal evaporation, it was found that the silicon substrate was deposited with white product. The morphology

* Address correspondence to these authors. E-mail: gzshen@ustc.edu and cjlee@hanyang.ac.kr.
† National Institute for Materials Science.
‡ Hanyang University.

10.1021/jp051078a CCC: $30.25
Published on Web 04/30/2005

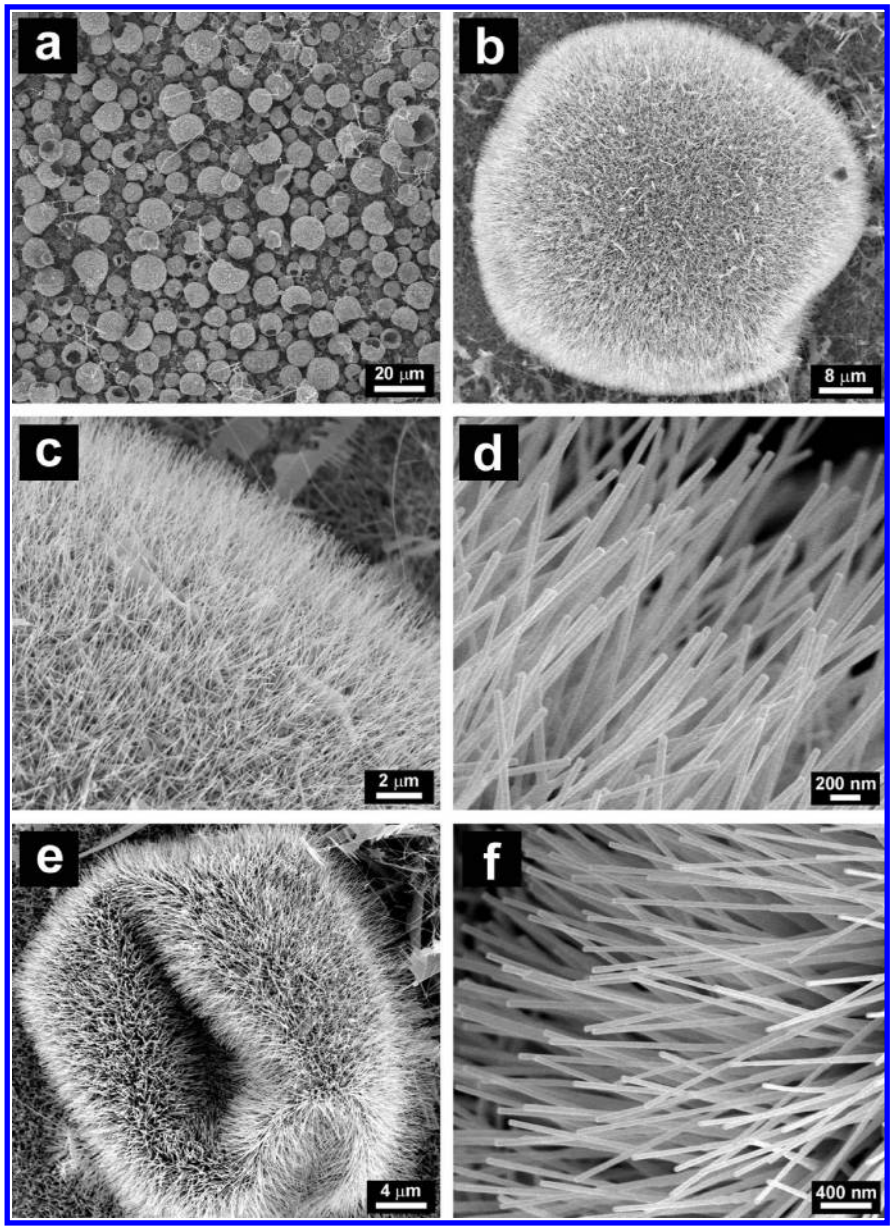

Figure 1. (a) A typical low-magnification SEM image of the as-synthesized hollow ZnO urchins on the substrate surface. (b−d) SEM images with different magnifications of a single ZnO urchin showing high-density ZnO nanowires with uniform diameter of about 40 nm radially aligned on the sphere surface. (e) SEM image of a typical hollow ZnO urchin showing the hollow cavities. (f) High-magnification SEM image of the ZnO nanowires grown on the urchin.

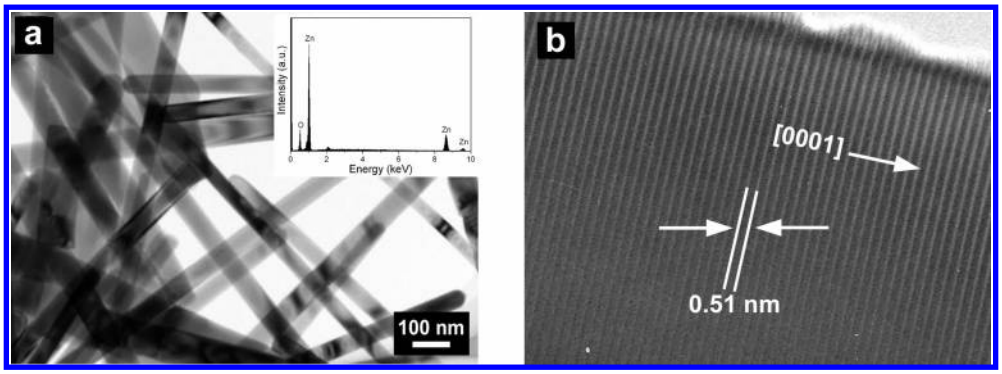

Figure 2. (a) TEM image of ZnO nanowires broken from the hollow ZnO urchins. (b) HRTEM image of the ZnO nanowire, indicating the [0001] growth direction.

of the product obtained after thermal evaporation for 60 min is shown in Figure 1.

Figure 1a is a low-magnification scanning electron microscopy (SEM) image which clearly shows that the whole substrate is covered with ZnO microspheres with diameters ranging from several to several tens of micrometers. The obtained ZnO microspheres indicate interesting hollow structures and the cavities of the spheres can be clearly seen from the SEM

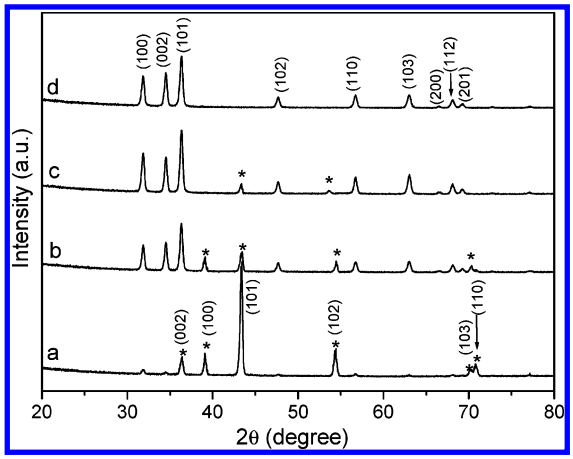

Figure 3. Evolution of XRD patterns from metallic Zn powder to hollow ZnO urchins at different reaction times: (a) 10 min; (b) 20 min; (c) 30 min; and (d) 60 min.

observation. Figure 1b is the SEM image of a single ZnO microsphere with a diameter of about 50 μm. It shows that numerous one-dimensional nanowires with very high density growth pointing toward the center of the sphere. This novel structure looks like the natural sea urchin, so we call it hollow ZnO urchin. The urchin-like structure is shown more clearly in high-magnification SEM images in Figure 1c,d, which indicate acicula crystallites radiating from the "urchin" center in a uniform size distribution. The ZnO nanowires grown from the center have uniform diameters and lengths of about 40 nm and 4 μm, respectively. Panels e and f of Figure 1 show the SEM images of different magnifications of a single hollow ZnO urchin showing clearly the hollow cavity. Undoubtedly, the hollow ZnO urchin also consists of numerous ZnO nanowires 40 nm in diameter and 4 μm in length radially grown from the center as discussed above.

Transmission electron microscopy (TEM) studies were carried out to examine the crystallography and structure of the hollow

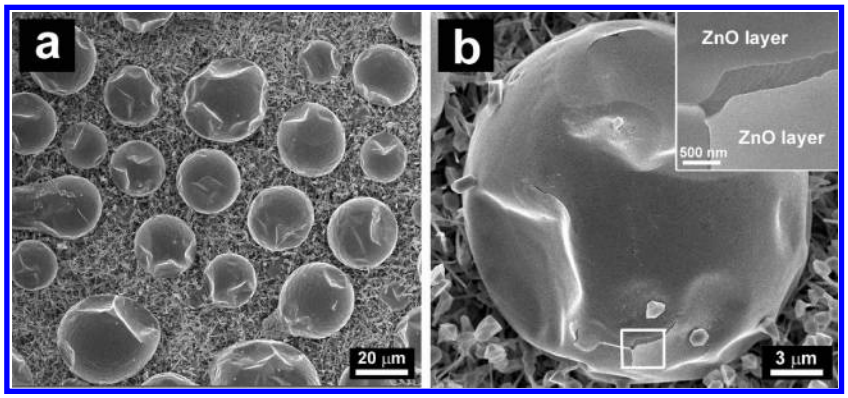

Figure 4. SEM images of the product after the thermal evaporation was performed for 10 min, showing the formation of Zn spheres with a thin layer of ZnO on the surface.

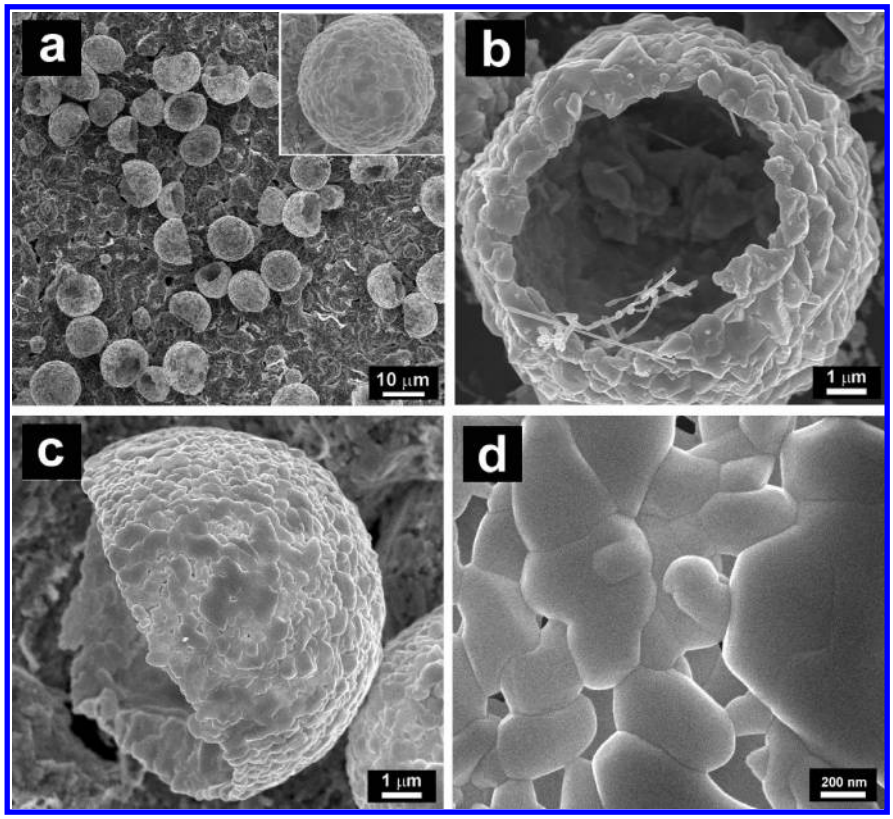

Figure 5. SEM images of the product after the thermal evaporation was performed for 20 min, showing highly rough hollow spheres are formed and many ZnO islands sprout from the surface.

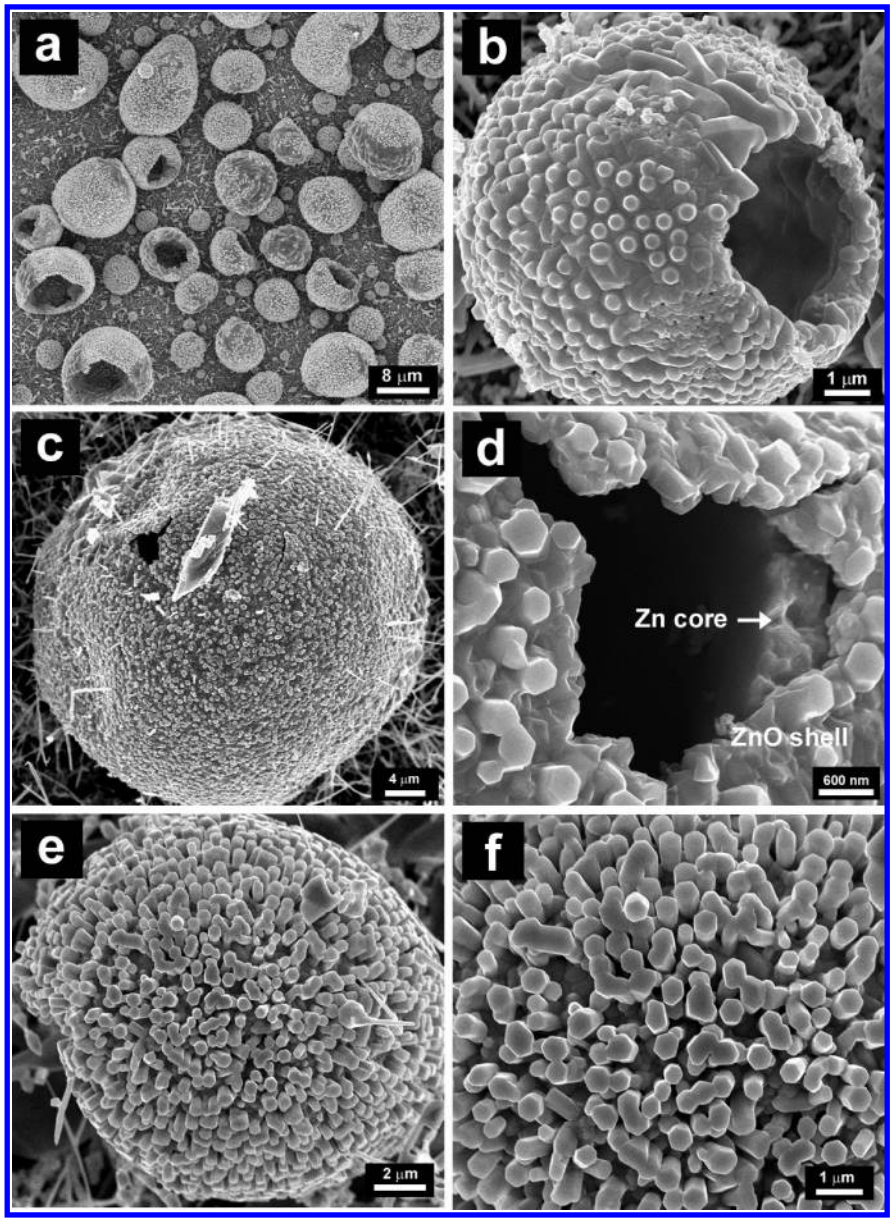

Figure 6. SEM images of the product after the thermal evaporation was performed for (a−d) 30 min, showing small ZnO nanorods grown from the islands (the Zn core is still clearly seen from the broken part of the sphere), and (e, f) 40 min, showing that small ZnO nanorods growing longer.

ZnO urchins. Figure 2a is the low-magnification TEM image of the ZnO nanowires broken from the hollow urchins after sonication treatment in ethanol for 1 h. It indicates that the ZnO nanowires are quite straight and have uniform diameters along their lengths. The diameters of the nanowires are about 40 nm in accordance with the SEM observations. The energy-dispersive X-ray spectrum (EDS) (Figure 2a, inset) recorded from the edge of the nanowire shown in Figure 2a indicates the presence of only Zn and O. Figure 2b is the lattice-resolved HRTEM image of a single ZnO nanowire. The lattice fringe of the ZnO nanowire is about 0.51 nm, corresponding to the (001) fringe perpendicular to the growth direction, which is consistent with that of the bulk wurtzite ZnO crystal.

X-ray diffraction (XRD) studies were performed of the products after thermal evaporation of zinc powder for different times to obtain information about the evolution of the phase transformation from Zn powder to hollow ZnO urchins. Figure 3 shows the series of XRD patterns of the products obtained at 10, 20, 30, and 60 min. After evaporation for 10 min, all the strong peaks on the XRD pattern (Figure 3a) marked with stars can be indexed to the hexagonal structure of Zn (JCPDS Card, No. 87-0713). On the same pattern, some weak peaks are also detected, which can be indexed to the hexagonal wurtzite ZnO phase (JCPDS Card, No. 36-1451). Since we use only metallic zinc powder in the experiment, the appearance of the ZnO phase indicates that Zn has been partially oxidized into ZnO. With

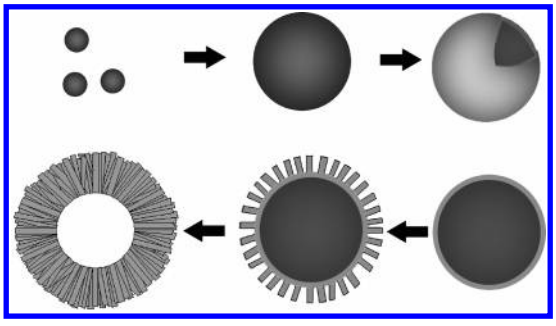

Figure 7. Schematic illustration of the formation of hollow ZnO urchins: the process involves the formation of Zn spheres on silicon substrate, oxidation of the spheres to form a thin layer of ZnO, sprouting of small ZnO nanorods, continuous evacuation of the Zn core, and finally the growth into ZnO urchins.

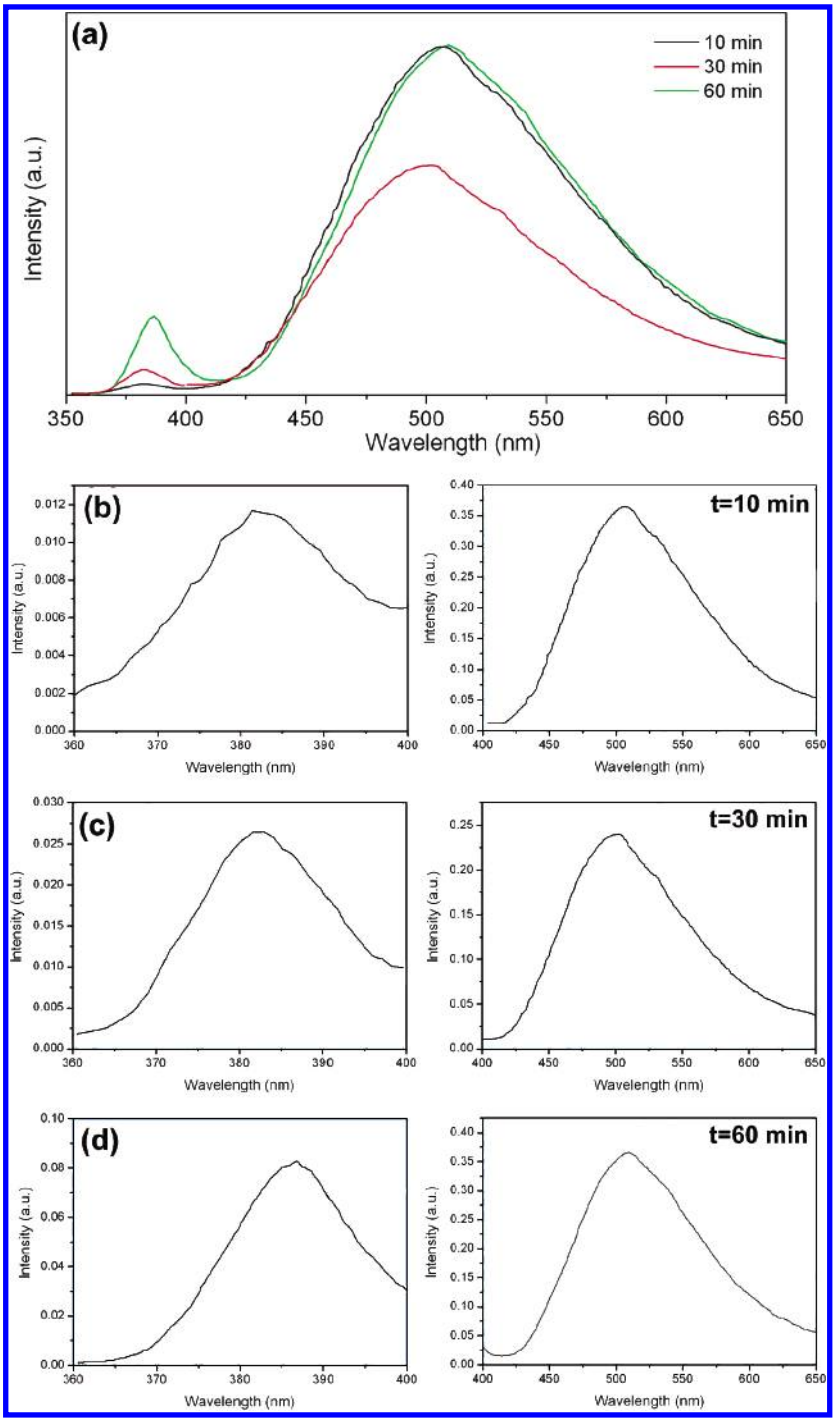

Figure 8. Evolution of room-temperature PL spectra, showing the increase of the relative intensity of UV emission to green emission with the increase of reaction time: (a) full spectra and (b−d) UV region and green region for different samples.

the increase of reaction time, the peak intensity of the ZnO phase increased gradually (Figure 3b,c), and after 60 min, all the peaks in the XRD pattern (Figure 3d) are of ZnO and can be readily indexed as the hexagonal wurtzite ZnO phase with cell constants $a = 3.248$ Å and $c = 5.204$ Å, which are in good agreement with the reported data in the literature (JCPDS Card, NO. 36-1451). The XRD pattern of the product obtained after 60 min indicates that Zn has been completely transformed into ZnO, which is in good agreement with the TEM and EDS results.

To further study the growth process from metallic Zn powders to hollow ZnO urchins, SEM studies were carried out for the products obtained at different reaction time. Figure 4a shows the low-magnification SEM image of the product obtained after 10 min, which shows that spheres with a very smooth surface are deposited on the substrate. XRD and EDX analyses indicate that they are Zn spheres wrapped with a thin layer of ZnO. Figure 4b shows a single Zn sphere 20 μm in diameter. The ZnO layer on the surface of the sphere can be clearly seen from the enlarged part shown in the inset in Figure 4b. Interestingly, parts of the spheres collapsed and even the inner Zn core was clearly seen under SEM observations.

After evaporation for 20 min, hollow Zn/ZnO core−shell spheres are obtained (Figure 5a). Since Zn has a much lower melting point of 419 °C, further thermal evaporation led to the sublimation of the Zn core and the shell collapsed and formed the hollow core−shell structures. Panels b and c of Figure 5 are SEM images of a single hollow Zn/ZnO core−shell sphere. The spheres show a much rougher surface compared with the

Zn spheres obtained after 10 min. On the spheres, many little ZnO islands sprouted from the surface and these islands are clearly seen from the high-magnification image shown in Figure 5d.

Further evaporation led to the formation of small ZnO nanorods epitaxially grown from the preformed ZnO islands on the sphere surfaces as shown in Figure 6. The small ZnO nanorods are of hexagonal cross-section 200−300 nm in diameter and 100−200 nm in length. The hexagonal cross-section of the nanorods indicates that they grow along the (001) direction, which is the common growth direction for one-dimensional wurtzite ZnO nanostructures. Figure 6d is the high-magnification SEM image of the broken part shown in Figure 6c. The inner Zn core is still clearly seen as indicated with an arrow. With the increase of evaporation time, more Zn was evaporated and the small ZnO nanorods grow longer (Figure 6e,f, 40 min). And after 60 min, all the inner Zn parts were depleted and the hollow ZnO urchins with high-density nanowires grown on the surfaces are formed just as discussed in Figure 1.

On the basis of the above analyses, we proposed the possible growth mechanism as follows. During the synthesis, Zn powder is initially heated to generate Zn vapors, which are transferred to the low-temperature region by Ar gas. Due to the high evaporation temperature, the concentration of the Zn vapor increases quickly and Zn atoms quickly condense and form liquid clusters in the low-temperature region. The liquid Zn droplets deposited on the substrate then quickly solidify to form Zn spheres. The surface of the Zn spheres can be easily oxidized by the residual oxygen in the system and form a thin ZnO layer on the Zn sphere surface. The inner Zn is further evaporated and deposited on the Zn sphere surface and oxidized into ZnO and ZnO islands formed on the surface due to the large lattice mismatch in the basal plane between Zn and ZnO. With prolonged reaction, small ZnO nanorods sprout out epitaxially from the surface via a self-catalytic mechanism[18,19] and finally Zn is depleted and hollow ZnO urchins are formed. The whole process can be illustrated as shown in Figure 7. The growth of hollow ZnO urchins was comprised of vaporization of Zn powder, solidification of liquid droplets, surface oxidation, sublimation, and self-catalytic growth of one-dimensional nanowires.

The products obtained at different reaction times are also studied by room-temperature photoluminescence (PL) analysis and it was found that evolution of the morphologies from Zn spheres to hollow ZnO urchins during the thermal evaporation process accompanied improvement of crystal qualities as reflected in the emission characteristics in the PL spectra.

Panels a−d of Figures 8 show the PL spectra of the products obtained at 10, 30, and 60 min, respectively. From the full spectra, it is clear that all the spectra of different products show a weak and sharp UV emission at ∼380 nm and a broad and strong green emission at ∼500 nm. To clearly show the relative intensity of the UV emission and the green emission, we separately show the emissions just as shown in Figure 8b−d. According to the literature, the UV emission with a peak at ∼380 nm corresponds to the near band edge (NBE) peak that is responsible for the recombination of free excitons of ZnO.[20] The broad and strong green emission at ∼500 nm obviously originates from the recombination of the holes with the electrons occupying the singly ionized oxygen vacancy.[15,21,22] From the PL spectra, the relative intensity of green emission to UV emission is 22 for the product after evaporation for 10 min, 9 for 30 min, and 4 for 60 min. The decrease of the relative intensity of green emission to UV emission with the increase of reaction time indicates the great improvement in crystalline quality from previous reports. Besides the decrease of the intensity of green emission to UV emission, it was also found that the green emission for the products obtained at different times became much stronger, indicating an increasing number of defects. This may result from the oxygen deficiencies at the increased surface area of ZnO nanorods and more interfaces with the core part with the evolution from Zn spheres to hollow ZnO urchins with high-density ZnO nanowires on the surfaces.

Conclusion

In summary, novel hollow ZnO urchins were synthesized by using a very simple atmospheric pressure thermal evaporation process on silicon substrate with zinc powder as the source material. The hollow ZnO urchins are composed of a large cavity and numerous ZnO nanowires expitaxially grown on the surface with very high density. These novel nanostructures may find uses in a variety of areas such as the fabrication of advance electronic and optoelectronic nanodevices.

References and Notes

(1) (a) Li, M.; Schnablegger, H.; Mann, S. *Nature* **1999**, *402*, 393. (b) Peng, X. G.; Manna, L.; Yang, W. D.; Wickham, J.; Scher, E.; Kadavanich, A.; Alivisatos, A. P. *Nature* **2000**, *404*, 59.

(2) (a) Whitesides, G. M.; Grzybowski, B. *Science* **2002**, *295*, 2418. (b) Pileni, M. P. *J. Phys. Chem. B* **2001**, *105*, 3358. (c) Colfen, H.; Mann, S. *Angew. Chem., Int. Ed.* **2003**, *42*, 2350.

(3) (a) Manna, L.; Scher, E. C.; Alivisatos, A. P. *J. Am. Chem. Soc.* **2000**, *122*, 12700. (b) Lee, S. M.; Jun, Y.; Cho, S. N.; Cheon, J. *J. Am. Chem. Soc.* **2002**, *124*, 11244.

(4) (a) Wu, Y.; Yan, H.; Huang, M.; Messer, B.; Song, J. H.; Yang, P. D. *Chem. Eur. J.* **2002**, *8*, 1260. (b) Shi, H. T.; Qi, L. M.; Ma, J. M.; Cheng, H. M.; Zhu, B. Y. *Adv. Mater.* **2003**, *15*, 1647. (c) Shen, G. Z.; Lee, C. J. *Cryst. Growth Des.* **2005**, in press.

(5) (a) Caruso, F.; Caruso, R. A.; Mohwald, H. *Science* **1998**, *282*, 1111. (b) Liu, B.; Zeng, H. C. *J. Am. Chem. Soc.* **2004**, *126*, 8124. (c) Sun, Y.; Xia, Y. *Science* **2002**, *298*, 2176.

(6) (a) Goldberger, J.; He, R.; Zhang, Y.; Lee, S.; Yan, H.; Cho, H. J.; Yang, P. *Nature* **2003**, 422, 599. (b) Liu, B.; Zeng, H. C. *J. Am. Chem. Soc.* **2004**, *126*, 16744.

(7) (a) Rodriguez, J. A.; Jirsak, T.; Dvorak, J.; Sambasivan, S.; Fischer, D. J. *J. Phys. Chem. B* **2000**, *104*, 319. (b) Minne, S. C.; Manalis, S. R.; Quate, C. F. *Appl. Phys. Lett.* **1995**, *67*, 3918.

(8) Huang, M.; Mao, S.; Feick, H.; Yan, H.; Wu, Y.; Kind, H.; Weber, E.; Russo, R.; Yang, P. *Science* **2001**, *292*, 1897.

(9) (a) Chang, P. C.; Fan, Z. Y.; Wang, D. W.; Tseng, W. Y.; Chiou, W. A.; Hong, J.; Lu, J. G. *Chem. Mater.* **2004**, *16*, 5133. (b) Kong, X. Y.; Ding, Y.; Yang, R. S.; Wang, Z. L. *Science* **2004**, *303*, 1348.

(10) Hu, P.; Liu, Y.; Wang, X.; Fu, L.; Zhu, D. *Chem. Commun.* **2003**, 1304.

(11) Gao, P.; Wang, Z. L. *J. Phys. Chem. B* **2002**, *106*, 12653.

(12) Lao, J. Y.; Wen, J. G.; Ren, Z. F. *Nano Lett.* **2002**, *12*, 1287.

(13) Lao, J. Y.; Huang, J. Y.; Wang, D. Z.; Ren, Z. F. *Nano Lett.* **2003**, *3*, 235.

(14) Gao, P.; Wang, Z. L. *J. Am. Chem. Soc.* **2003**, *125*, 11299.

(15) (a) Pan, Z. W.; Dai, Z. R.; Wang, Z. L. *Science* **2001**, *291*, 1947. (b) Huang, M.; Wu, Y.; Feick, H.; Tran, N.; Weber, E.; Yang, P. *Adv. Mater.* **2001**, *13*, 113. (c) Hu, J. Q.; Bando, Y. *Appl. Phys. Lett.* **2003**, *82*, 1401.

(16) (a) Zhang, J.; Sun, L.; Liao, C.; Yan, C. *Chem. Commun.* **2002**, 262. (b) Vayssieres, L. *Adv. Mater.* **2003**, *15*, 464.

(17) (a) Lee, C. J.; Lee, T. J.; Lyu, S. C.; Zhang, Y.; Ruh, H.; Lee, H. J. *Appl. Phys. Lett.* **2002**, *81*, 3648. (b) Shen, G. Z.; Cho, J. H.; Jung, S. I.; Lee, C. J. *Chem. Phys. Lett.* **2005**, *401*, 529. (c) Lyu, S. C.; Zhang, Y.; Lee, C. J. *Chem. Mater.* **2003**, *15*, 3294. (d) Shen, G. Z.; Cho, J. H.; Jung, S. I.; Yoo, J. K.; Yi, G. C.; Lee, C. J. *J. Phys. Chem. B* **2005**, *109*, 2005.

(18) Yao, B. D.; Chan, Y. F.; Wang, N. *Appl. Phys. Lett.* **2002**, *81*, 757.

(19) Yu, W. D.; Li, X. M.; Gao, X. D. *Appl. Phys. Lett.* **2004**, *84*, 2658.

(20) Kong, Y. C.; Yu, D. P.; Zhang, B.; Fang, W.; Feng, S. Q. *Appl. Phys. Lett.* **2001**, *78*, 407.

(21) Vanheusden, K.; Warren, W. L.; Seager, C. H.; Tallant, D. R.; Voigt, J. A.; Gnade, B. E. *J. Appl. Phys.* **1996**, *79*, 7983.

(22) Wu, X. L.; Siu, G. G.; Fu, C. L.; Ong, H. C. *Appl. Phys. Lett.* **2001**, *78*, 2285.